Available online at www.sciencedirect.com
ScienceDirect
C. R. Physique 8 (2007) 221–233
COMPTES RENDUS PHYSIQUE
http://france.elsevier.com/direct/COMREN/

Recent advances in crystal optics/Avancées récentes en optique cristalline

Quadratic spatial solitons

George I. Stegeman

College of Optics and Photonics/CREOL, University of Central Florida, 4000 Central Florida Boulevard, Orlando, FL 32816-2700, USA

Available online 7 August 2006

Invited Paper

Abstract

Quadratic spatial solitons, beams that propagate unchanged in shape and magnitude, are supported by second order optical nonlinearities and can occur in all wave mixing processes under appropriate conditions. They are multi-component, consisting of all the frequency components that are coupled by a second order nonlinear interaction near a phase-matching condition. They have been observed in a number of bulk crystalline media, in $LiNbO_3$ slab waveguides and in arrays of parallel, weakly coupled, $LiNbO_3$ channel waveguides. The properties of the solitons and their excitation will be reviewed. ***To cite this article: G.I. Stegeman, C. R. Physique 8 (2007).***

Résumé

Solitons spatiaux quadratiques. Les solitons spatiaux quadratiques, rayons qui se propagent à forme et amplitude constantes, sont gouvernés par les non-linéarités optiques du deuxième ordre et peuvent, dans des conditions appropriées, se produire dans tous les processus de mélange d'ondes. Ils sont multi-composantes, constitués de toutes les composantes fréquentielles qui sont couplées par une interaction non linéaire du deuxième ordre au voisinage d'une condition d'accord de phase. Ils ont été observés dans un certain nombre de milieux cristallins en volume, de guides d'ondes planaires en $LiNbO_3$ et sur des ensembles de guides d'ondes canaux en $LiNbO_3$, parallèles et faiblement couplés. Cet article fait le point sur les propriétés des solitons et leur processus d'excitation. ***Pour citer cet article : G.I. Stegeman, C. R. Physique 8 (2007).***

Keywords: Soliton; Quadratic spatial solitons

Mots-clés : Soliton ; Solitons spatiaux quadratiques

1. Introduction

In the evolution of nonlinear optics, second order nonlinear interactions (via the susceptibility $\chi^{(2)}$) have been primarily concerned with generating new frequencies as efficiently as possible. Second harmonic generation (SHG) in which the frequency of an input wave is doubled is by far the most frequent application since the inception of the field in the 1960s [1]. Sum (SFG) and difference (DFG) frequency generation of two input beams of different frequency has also been important, primarily because these two processes are the basis for optical parametric generation (OPG) and amplification (OPA) [2]. These processes and their applications are dealt with in detail elsewhere in this special issue.

E-mail address: george@creol.ucf.edu.

1631-0705/$ – see front matter
doi:10.1016/j.crhy.2006.02.008

Here the focus will be on a phenomenon well-known in wave science that all nonlinearities can support waves that propagate without change in their shape and peak amplitude, i.e., spatial solitons [3]. The early history of spatial solitons in optics has been dominated by investigations in Kerr or Kerr-like materials that support mono-frequency solitons [4–7]. In Kerr media which can be defined by a local index change Δn linear in the local intensity (i.e., $\Delta n = n_2 I$), self-focusing of beams is known to occur for $n_2 > 0$. Bright Kerr solitons exist when this self-focusing process is balanced by linear diffraction. In this case the diffraction referred to is in the plane of the waveguide and is quantified by the diffraction length L_d. There is also a characteristic nonlinear length L_nl defined approximately by the distance that the beam propagates to acquire a maximum nonlinear phase shift $\Delta\phi^\mathrm{NL} \cong \pi/2$ where $\Delta\phi^\mathrm{NL} = k_\mathrm{vac} n_2 I$. Spatial solitons can exist when $L_\mathrm{nl} \leqslant L_\mathrm{d}$, i.e., when the nonlinear process is dominant. *But*, such Kerr bright solitons can only exist in slab waveguides (1D) [8]. Bulk Kerr media for which beams diffract in two spatial directions do not support spatial solitons [8]. However, for any departure from the $\Delta n = n_2 I$ behavior, usually due to the saturation of an electronic transition, bulk media do support 2D solitons and these have been observed [9]. Other nonlinear materials in which bright spatial solitons have been observed in either 1D or 2D include photorefractive materials, liquid crystals, active semiconductors, etc. [10–13].

For quadratically nonlinear media, it is known that there are mechanisms that effectively lead to self-focusing of beams [14]. For example, for SHG it is known that nonlinear phase shifts are accumulated on propagation due to 'cascading' in $\chi^{(2)}$, similar to those obtained in self-focusing Kerr media [15]. Furthermore, the nonlinear polarization induced is given, for example for Type I second harmonic generation (SHG), by

$$P^\mathrm{NL} = \varepsilon_0 \chi^{(2)}_\mathrm{eff}\left[E^2(\omega) + 2E(2\omega)E^*(\omega)\right] \tag{1}$$

where $\chi^{(2)}_\mathrm{eff}$ is the effective second order susceptibility for the particular interaction. Both the sum $[E^2(\omega)]$ and difference $[E(2\omega)E^*(\omega)]$ frequency processes are proportional to the product of two optical fields. Assuming beams of finite transverse cross-section, the resulting nonlinear polarization source P^NL is narrower in space than either of the two fields and it generates narrowed fields at 2ω and ω respectively. Thus the total beams are narrowed on propagation. These narrowing processes can counteract diffraction, leading to solitonic propagation. Based on these processes, quadratic spatial solitons have been observed in $\chi^{(2)}$-active slab waveguides and bulk media [16–23]. The newest geometries in which quadratic solitons have been observed have utilized arrays of weakly coupled channel waveguides [24,25]. A selection of all of these cases, chosen to describe some fundamental properties, will be reviewed in this article.

2. 1D (slab waveguide) quadratic solitons

2.1. Theory

The discussion here will be focused on the simplest case of SHG in Type I or QPM (Quasi-Phase-Matched) configurations. Similar but more complicated results are obtained for Type II geometries, SFG, DFG, OPGs and OPAs [26]. The coupled wave equations, including 1D diffraction, are well known for Type I or QPM SHG [27]. Considering the simplest case of a 1D slab waveguide with propagation along the z-axis and diffraction along the y-axis,

$$\begin{aligned} &\mathrm{i}\frac{\partial}{\partial z}a_2(y,z) - \frac{1}{2k_2}\frac{\partial^2}{\partial y^2}a_2(y,z) - \Gamma a_1^2(y,z)\exp[-\mathrm{i}\Delta k z] = 0 \\ &\mathrm{i}\frac{\partial}{\partial z}a_1(y,z) - \frac{1}{2k_1}\frac{\partial^2}{\partial y^2}a_1(y,z) - \Gamma a_1^*(y,z)a_2(y,z)\exp[\mathrm{i}\Delta k z] = 0 \end{aligned} \tag{2}$$

with the normalized (to unity power) fundamental ($p = 1$) and harmonic ($p = 2$) fields given by a_p, k_p are the guided wave propagation wave vectors with $\Delta k = 2k_1 - k_2$, and $\Gamma \propto \chi^{(2)}_\mathrm{eff}$ [27]. Here $\chi^{(2)}_\mathrm{eff}$ depends on the polarizations of the interacting waves and is averaged by an overlap integral over the x-direction of the waveguide.

These equations, subject to the condition $\partial|a_p|/\partial z = 0$, do not have analytical solutions except for two very special cases and need to be solved numerically to find the solitons which are the *nonlinear* eigenmodes of the SHG process [28,29]. They satisfy the nonlinear polarization driven wave equation for each of the frequency components coupled together via $\chi^{(2)}$. For a given wavevector mismatch and total power there will be a unique spatial soliton. Thus there are two governing parameters. For each of these parameters there are specific amplitudes, spatial widths and relative

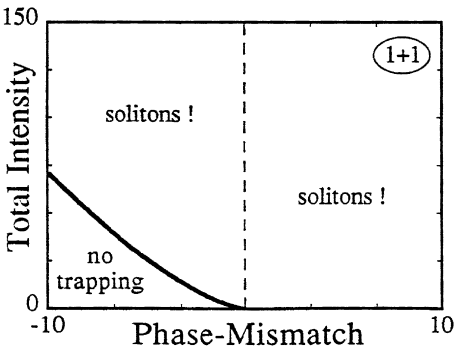

Fig. 1. The energy versus normalized wavevector mismatch existence diagram for 1D (slab waveguide) Type I quadratic spatial solitons.

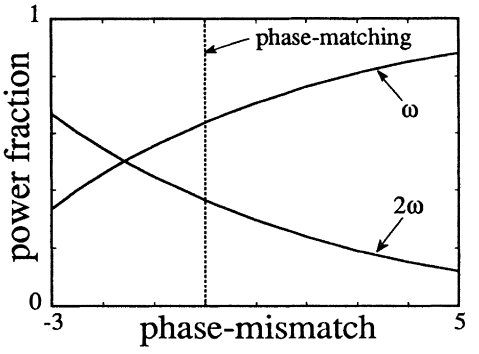

Fig. 2. Variation in the fraction of power carried by the fundamental (ω) and harmonic (2ω) components of a 1D quadratic soliton versus the normalized wavevector mismatch.

phases associated with each of the frequency components present in the soliton. For Type I or Quasi-phase-matched (QPM) SHG geometries the steady state solutions consist of *in phase* fundamental and harmonic fields. Note that this contrasts strongly with the case of efficient frequency conversion, for example for SHG, which is optimized for a $\pi/2$ phase shift between the two fields. Furthermore, there is an additional nonlinear phase contribution to both steady state fields which is linear with distance. It occurs under all phase-matching conditions [30,31]. This can be considered to be an additional contribution to the propagation wave vectors. In fact, the only way to lock the two fields to be always in phase even when there is an initial linear wavevector mismatch is for the effective nonlinear contributions to the propagation wave vectors to be sufficiently different to also cancel out that initial linear wavevector mismatch.

Numerical results for the key soliton properties are shown in Figs. 1 and 2 [32]. The regions of parameter space (normalized wavevector mismatch versus soliton intensity) that can support 1D quadratic solitons are shown in Fig. 1. Quadratic solitons can exist at all intensities for positive wavevector mismatch and for negative wavevector mismatches above the solid line. Note that these thresholds are for the steady state solutions. The ratio of the peak amplitudes of the two fields changes with wavevector mismatch. This behavior shown in Fig. 2 is typical, i.e., as the wavevector mismatch decreases to zero and becomes progressively more negative, the fundamental contribution decreases and the harmonic component increases. For large positive wavevector mismatch when the harmonic is negligibly small, this is the so-called Kerr or cascading limit in which the second order interaction leads to an effective Kerr nonlinearity given by $n_{2,\mathrm{eff}} = 2k_{\mathrm{vac}}[\chi^{(2)}_{\mathrm{eff}}]^2/\varepsilon_0 cn^3\Delta k$ and the solutions approach asymptotically those for 1D Kerr solitons.

The steady state soliton solutions can be optimally excited at the input to a sample by injecting both the fundamental and harmonic in the proper ratio, and in phase [18]. The quadratic solitons are 'robust' in the sense that any strong excitation of the fundamental and harmonic will evolve into the solitons, providing the initial conditions contain enough total power for a soliton to exist. If they were not robust and instead required very well specified initial conditions on the fields, they would be very difficult to excite. In fact, experimentally it is easier to inject only the fundamental and rely on the fact that second harmonic can be generated with distance down the waveguide. The problem, of course, is that the second harmonic will initially be $\pi/2$ out of phase with the fundamental where-as the quadratic soliton require in-phase fields. Because the solitons are the nonlinear eigenmodes of the nonlinear medium, the magnitude, width and phase of the generated harmonic field evolves with distance into the soliton field [33,34]. This does not occur adiabatically and some fundamental and harmonic are radiated away. An example of how the magnitudes of the fields evolve is shown in Fig. 3 [17]. Note that there are radiation fields generated which propagate away from the region of the soliton resulting in net losses between the input power and the final soliton power. Hence the threshold intensities required for soliton excitation will be larger than those shown in Fig. 1. After a few diffraction lengths, a very good approximation to a quadratic soliton is obtained. In general, the larger the second harmonic needed, the longer the distance required for steady state to be reached by fundamental only excitation.

Having established the complexity of finding solutions and the field structure for quadratic solitons, the question is whether there are any simple approximate ways to determine the powers etc. required for soliton excitation? In fact one can develop "rule-of-thumb" estimates for the appropriate fundamental intensity incidence condition in terms

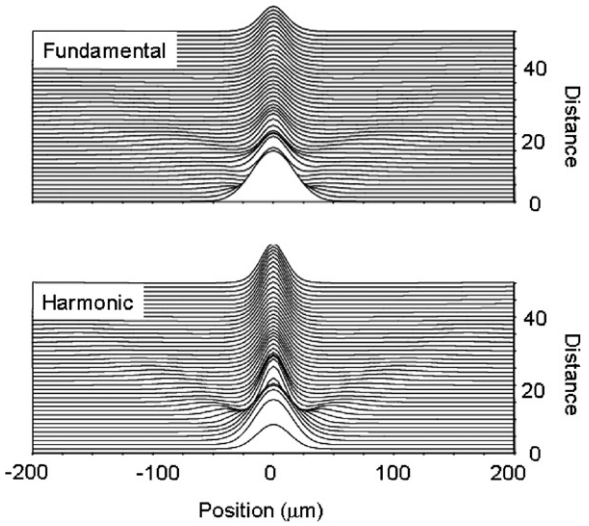

Fig. 3. Simulations of the evolution of both the fundamental and harmonic fields with propagation distance when a 1D quadratic soliton is excited by the fundamental field only.

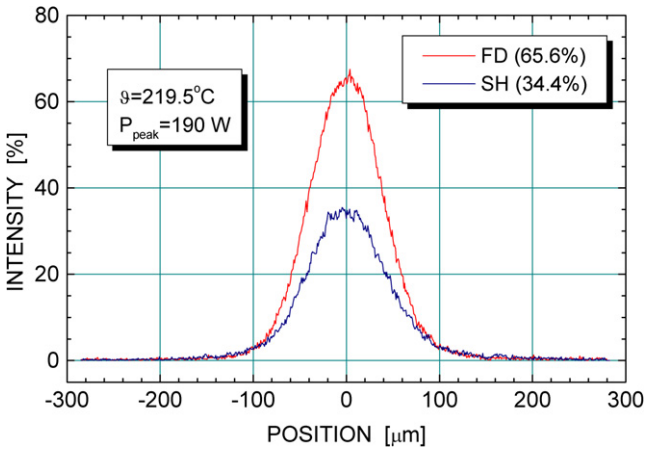

Fig. 4. The output beam profiles of the fundamental (FD) and second harmonic (SH) components of a 1D quadratic soliton from a QPM $LiNbO_3$ slab waveguide when excited right at phase-matching.

of the effective lengths associated with the different processes present. Quadratic solitons can be generated when $L_d \geqslant L_{coh} > L_{pg}$ where the diffraction length is $L_d = \pi w_0^2 n/\lambda$, L_{coh} is the coherence length associated with the wavevector mismatch $|\Delta k|$ and $L_{pg} \cong cn/2\omega\chi_{eff}^{(2)}|a_1(0,0)|$ is the parametric gain length associated with SHG, i.e., the distance required for a substantial exchange of energy between the two frequencies.

2.2. 1D quadratic solitons

Experiments have been reported in $LiNbO_3$ at 1550 nm with both Type I and QPM phase-matching using fundamental wave only excitation [16,17]. The sample length was 5 cm in these experiments and a narrow bandwidth pulsed laser with pulse width of about 8 ps was used. The most detailed work was done for the QPM case utilizing the large d_{33} coefficient and waveguides 5 cm long [17]. Shown in Fig. 4 are the intensity profiles of a soliton on phase-match [17]. As predicted in Fig. 2, the fundamental beam contains about twice the energy of the harmonic for this case. Note that the beam widths at the two frequencies are comparable for this case. What is most noteworthy is that, despite the fact that the harmonic was generated by the fundamental which usually leads to a distortion of the fundamental profile, both soliton components exhibit undistorted profiles. This is a direct consequence of soliton formation!

Additional experiments were performed at a fixed value of the phase (wavevector) mismatch, 7.1π, and increasing the input power [17]. The family of spatial solitons corresponding to a vertical slice in Fig. 1 was experimentally obtained and is shown in Fig. 5. Note that the vertical axes are quoted in terms of pulse energies because the high soliton powers required necessitated pulsed lasers. The trade-off between the soliton width and peak power is clear although the product is not a constant as it is in the Kerr case. Furthermore, it can also be seen that the lower the peak power of the soliton's fundamental, the weaker the harmonic component. The agreement between experiment and theory is good.

In a quadratic soliton the different frequency components are locked together in space, i.e., have the same direction for their group velocities. For the two $LiNbO_3$ geometries studied extensively, Type I and QPM, the solitons were generated primarily along a crystal axis so that the group velocities were collinear. However, by tuning the fundamental input direction away from a crystal axis by tilting the sample relative to the input beam, different group velocity directions can be induced for the fundamental and harmonic [35]. Shown in Fig. 6 are simulations for the fundamental and harmonic when the fundamental is excited at a few degrees from the crystal axis. At low powers, the fundamental would diffract and propagate in a direction orthogonal to the transverse axis. In Fig. 6(a), the direction that a soliton's fundamental beam propagates is shown to be deflected from the low power case. Fig. 6(b) reveals the direction into

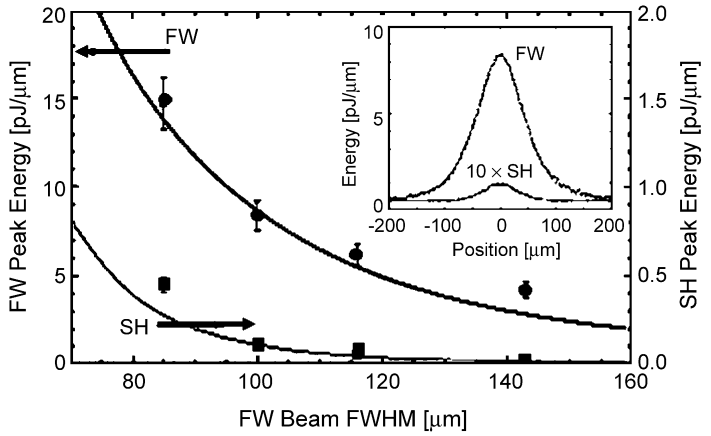

Fig. 5. The trade-off between the pulse energy in the fundamental (FW) and harmonic (SH) components of a 1D quadratic soliton and the full width half maximum width of the components for QPM $LiNbO_3$ slab waveguides at 1550 nm for a low power phase mismatch of 7.1π. Shown in the inset is a typical set of intensity profiles.

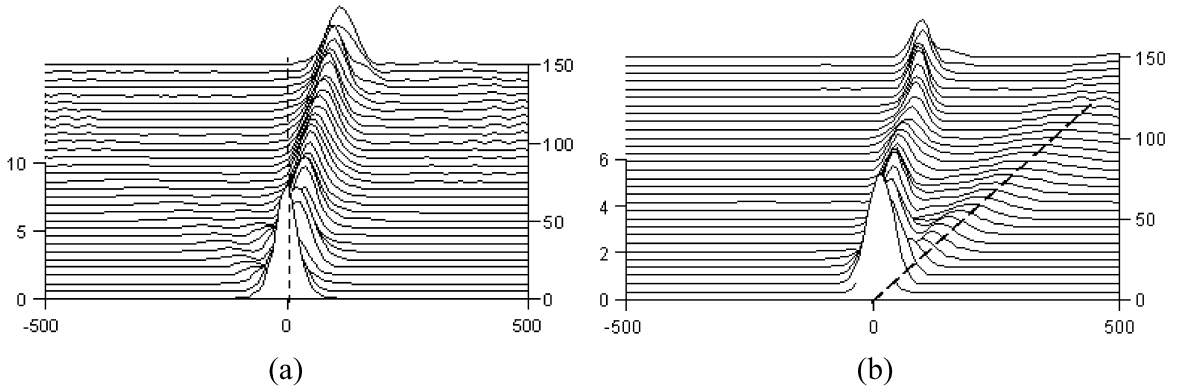

Fig. 6. Simulation of the propagation of (a) the fundamental beam and (b) the second harmonic of a quadratic soliton with walk-off. No seed beam for the second harmonic was launched. The weak, diffracting, freely propagating part of the second harmonic was radiated at the walk-off angle indicated by the dashed line in (b). A low power (no soliton locking) fundamental (not shown) propagated as shown by the dashed line in (a). Both the fundamental and second harmonic soliton components propagated together in a direction intermediate between the freely propagating fundamental and harmonic.

which the (non-soliton) freely propagating (and diffracting) harmonic component is radiated from the input interface and the direction of the soliton's harmonic component. At the high powers associated with soliton formation, the two beams are pulled towards each other where they spatially lock together and propagate in the same direction. The experimental deflection of the fundamental component of the soliton from the direction of the freely propagating fundamental beam is shown in Fig. 7 for three cases. Note that the walk-off length, L_w must be shorter than the L_{pg} for the spatial locking to take place.

When the power in an input fundamental beam of fixed width is increased to powers higher than those required for a single soliton, filamentation can eventually occur [36,37]. This occurs due to a process called 'modulational instability' and is a consequence of the same trade-offs between diffraction and self-focusing known for soliton formation. An example of the evolution is shown in Fig. 8 for a Type I birefringence phase-matched sample [37]. In Fig. 8(a), there are three superimposed curves. The input beam is the dashed line, the diffracted beam is the wide solid line and the soliton, obtained at an input power of 2.4 kW, is the solid dark line. Note that the low power tails of the soliton are wider and more intense than those on the input beam. This is a consequence of using pulsed excitation and these low power tails are too weak to participate in the soliton process and undergo linear diffraction. For peak input powers about twice the soliton power, a strong side lobe appears on each side of the main soliton peak, innermost curves in Fig. 8(b). These side lobes are not quite intense enough to form solitons and they eventually radiate away to the sides of the waveguide. At four times the soliton power, four peaks appear whose position and relative peak power varies

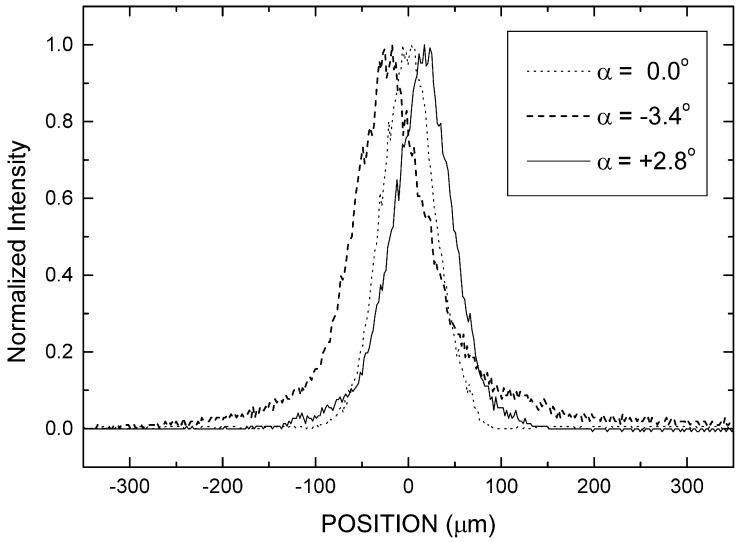

Fig. 7. Fundamental *output* beam profiles when a quadratic soliton is generated in a 1D $LiNbO_3$ slab waveguide along the crystal axis, and at angles (denoted by α) on either side of the crystal axis. The position zero corresponds to the output position of each low power fundamental, i.e., no soliton formation.

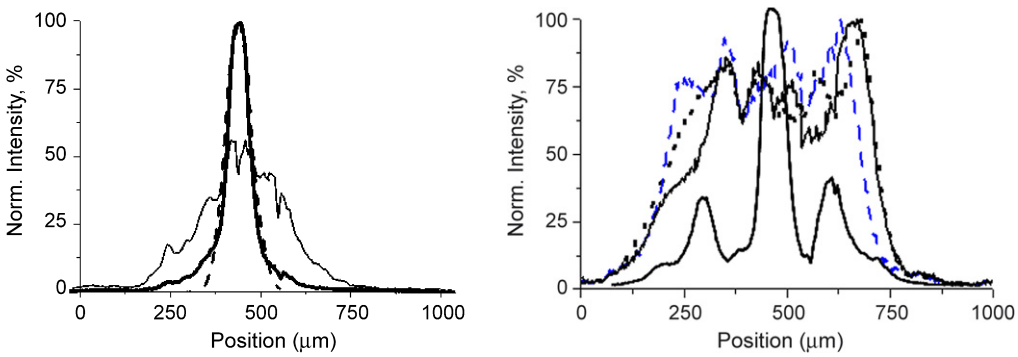

Fig. 8. Intensities of fundamental beam profiles. (a) Dashed line—a 74 μm wide FW input beam injected into a QPM Ti:indiffused, $LiNbO_3$ slab waveguide; wide dark line—diffracted beam; heavy dark line—1D quadratic spatial soliton. (b) Three-peaked line—output at twice the single soliton power threshold showing the soliton and two weaker filaments; similar dashed, dotted and solid lines—multi-filament outputs which vary from shot-to-shot.

from shot-to-shot of the pulsed laser. This corresponds to noise-initiated modulational instability which was predicted many years ago for the quadratic case [36]. More detailed experiments with much wider input beams have established that the spacing between the filaments decreases with increasing power and that the 'gain' coefficients associated with filament formation from noise agree well with theory [38]. For propagation distances much longer than the samples used, these beams would separate laterally and eventually evolve into individual solitons. For very wide input beams, many filaments occur and continue to interact semi-chaotically for long propagation distances [39]. In the infinitely wide beam case, these filaments never evolve into individual solitons.

2.3. Quadratic solitons in bulk media

The power versus wavevector of the soliton existence region for 2D is similar to the 1D case. The major difference is that the boundary of the existence region rises from zero at the origin with increasing positive wave vectors, as shown in Fig. 9 [40]. This last feature differs from the 1D case in which there is no threshold for positive wavevector mismatch. Most of the other properties such as the power and wavevector dependence of the beam composition,

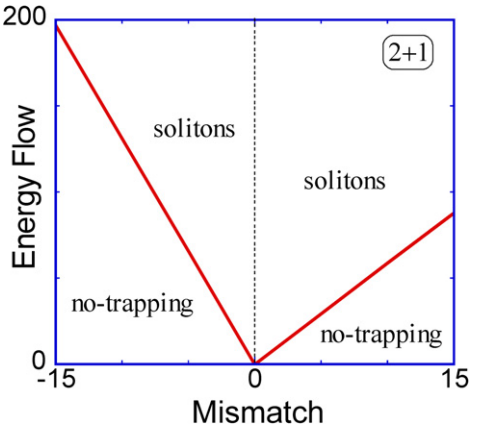

Fig. 9. The energy versus normalized wavevector mismatch existence diagram for 2D Type I quadratic spatial solitons in bulk media.

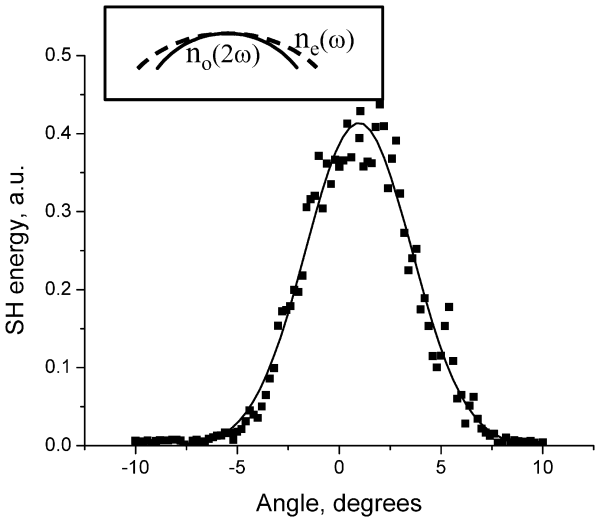

Fig. 10. The SHG angle tuning response of the $KNbO_3$ crystal versus angle of incidence for the NCPM geometry.

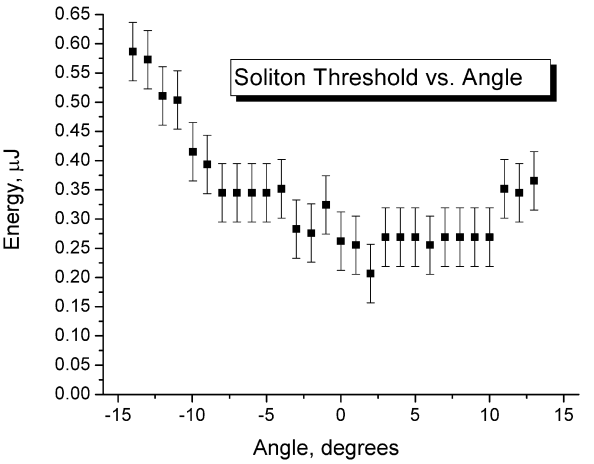

Fig. 11. The fundamental beam threshold (pulse energy) for the generation of NCPM quadratic solitons in $KNbO_3$ at 985 nm versus incidence angle.

widths, locking into a common propagation direction in the presence of walk-off, etc. are generically the same, although different in details [26,41]. Another interesting difference occurs due to the crystalline nature of many of the media used for second order nonlinear interactions, namely that diffraction is anisotropic. That is, a low power circular cross-section input beam evolves into an elliptic beam on propagation, which in turn leads to elliptically polarized spatial solitons at high powers [42,43]. The resulting soliton ellipticity is small and has not been measured yet. However, as will be discussed later, this crystal anisotropy impacts strongly the generation of multiple solitons with fundamental only inputs.

Many experiments on quadratic soliton generation were reported in the 1990s. The materials used were KTP, $LiIO_3$, BBO and periodically poled KTP and $LiNbO_3$ [18–23]. Fundamental wave only excitation was invariably used in SHG geometries. As mentioned previously, essentially any doubling crystal which can be used to demonstrate SHG will also lead to quadratic solitons at sufficiently high power levels. Discussed next will be a number of interesting peculiarities observed in experiments performed on bulk crystals.

A number of features were observed in experiments on non-critically phase-matched (NCPM) $KNbO_3$ [22]. Shown in Figs. 10 and 11 are measurements of the angle tuning dependence of the SHG response (bandwidth) at low powers for comparison with the bandwidth for soliton generation [22]. The NCPM SHG bandwidth is quite broad to start with, namely about 7 degrees. However, note that for the 1.1 cm long crystal the soliton threshold power bandwidth is

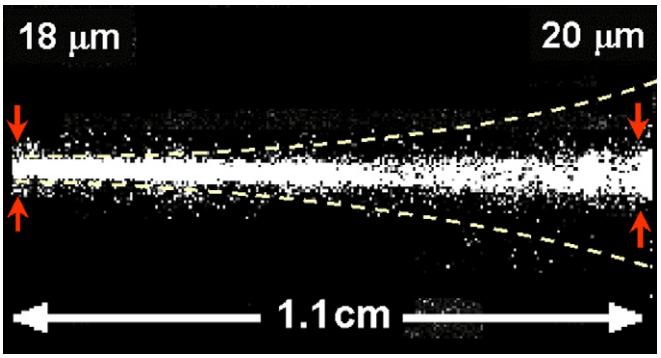

Fig. 12. Intensified image of a 985 NCPM quadratic soliton propagating in a NCPM $KNbO_3$ crystal, excited by a 36 GW/cm^2 incident beam.

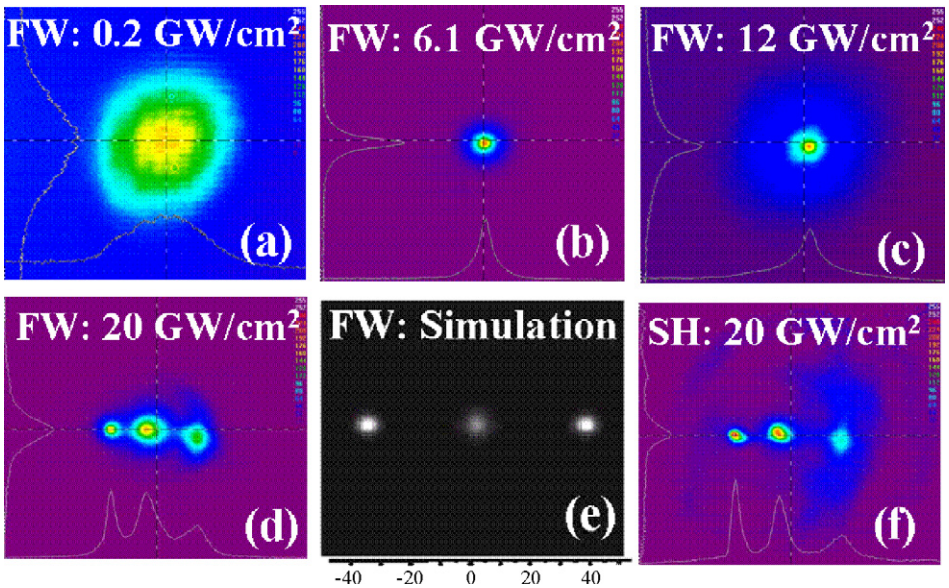

Fig. 13. (a) to (d) are output patterns from a NCPM PPKTP crystal at different input intensities of the 985 fundamental beam. (e) is a simulation for the conditions in (d). (f) is the harmonic intensity pattern corresponding to (d).

much larger, about 25 degrees. The reason is quite simple. The SHG bandwidth is associated with efficient generation integrated over the full crystal length which is then approximately equal to L_{pg}. However, a soliton is fully formed at the crystal's output facet and occurs at the much higher powers for which L_{pg} is only a fraction of the crystal length and the soliton bandwidth reflects this smaller L_{pg}.

Also obtained at very high powers in NCPM $KNbO_3$ was a direct image of quadratic soliton propagation inside the crystal [22]. It is shown, as photographed from above the crystal, in Fig. 12. In fact the scattering image had to be electronically intensified since it was just barely visible to the eye. The dashed lines have been added to show how the diffracting low power beam should appear. For that case the scattering was much too faint to be obtained.

Just as in the 1D case discussed previously, when the input fundamental beam power is increased beyond that needed for a single soliton, a form of filamentation and radiation losses also occur in 2D. Shown in Fig. 13 is a collage of outputs from a PPKTP crystal for increasing fundamental intensity input into the crystal on phase-match [43,44]. Fig. 13 (upper row) shows in sequence: (a) the fundamental diffracted beam, (b) the fundamental component of the spatial soliton just above threshold, and (c) the fundamental component of the spatial soliton at two times threshold with a 'halo' due to radiation around it. The appearance of two additional solitons at an input intensity three times that of the single soliton threshold is shown in Figs. 13(d) and (f) respectively [43,44]. These results are in excellent agreement with simulations of the propagation equations, as shown for the fundamental in Fig. 13(e).

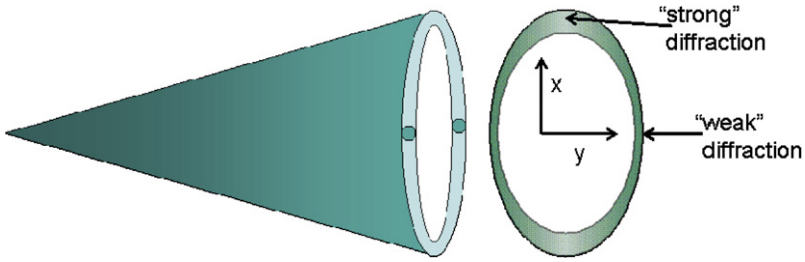

Fig. 14. Illustration of the radiation cones given off when quadratic solitons are excited with a fundamental only beam at input intensities above the single soliton threshold. The formation of solitons due to a coalescence of the fields are also shown along directions corresponding to the weakest diffraction.

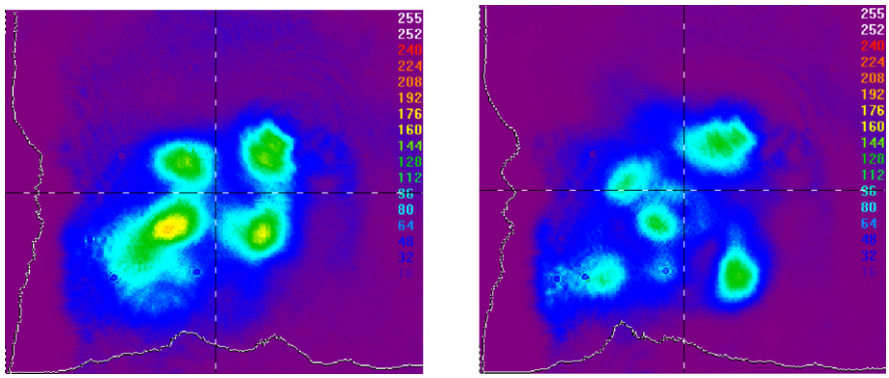

Fig. 15. Multifilament patterns observed from NCPM $KNbO_3$ at 985 nm with input fundamental intensities of 36 GW/cm^2.

The physics of multi-soliton generation can be easily understood from the simulations [43,45,46]. For fundamental beam excitation, both the fundamental and harmonic oscillate with propagation distance. This leads to the emission of radiation in the form of diverging cones, Fig. 14(a). Typically the first cone diverges very quickly where-as the second one (shown), generated some distance into the sample, diverges slowly. The crystal anisotropy leads to a preferred transverse axis along which the diffraction is smaller than the orthogonal axis, as indicated in Fig. 14(b). The simulations show that when the radiation is sufficiently intense, radiation along the axis exhibiting the slowest diffraction coalesces into additional solitons, leading to the three soliton pattern along a line [44,45]. Another effect which has been shown to lead to lines of multiple solitons is input beam asymmetry [45]. Since the rate of diffraction along a given axis is inversely proportional to the input beam size along that direction, solitons are expected to coalesce out of the radiation cones along the lines of the major axes of elliptical beam inputs. In fact that has also been demonstrated.

When input beams have peak intensities many times the threshold intensity for a spatial soliton corresponding to that input beam width, filamentation occurs driven by the noise on the input beams [46,47]. Examples of such filaments at input intensities ten times that of the soliton threshold are shown in Fig. 15 [47]. When the input is obtained from pulsed lasers whose noise distribution varies from pulse to pulse, the output patterns from the crystal also vary from shot-to-shot.

An important question is whether soliton generation is useful for efficient second harmonic generation, i.e., in commercial doublers. The largest advantage afforded by quadratic solitons is that the field profiles of all of the frequency components are essentially perfect [48]. However, the 'price to be paid' for this attractive feature is quite high. The structure of the solitons, i.e., the fundamental to harmonic ratio is fixed so that the maximum SH conversion is typically 50%. Furthermore, that conversion efficiency is achieved over only a fraction of the crystal length and the remaining length is used to reach a steady state soliton. Indeed, if efficient frequency conversion is the primary goal, soliton generation is not the optimum choice.

3. Discrete quadratic solitons

A new research direction has recently emerged in which spatial solitons have been investigated in discrete (instead of continuous) systems [49]. As has frequently occurred in the history of spatial solitons, the initial work was reported

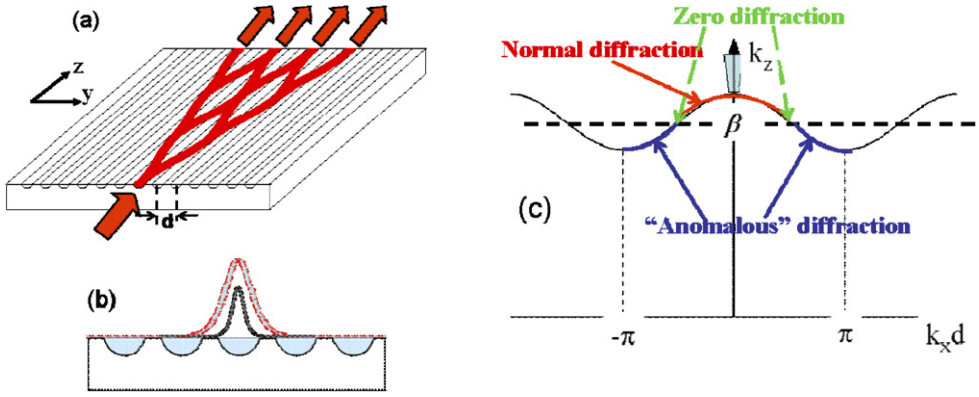

Fig. 16. (a) An array of parallel, weakly coupled PPLN waveguides. Also shown is the effect of discrete diffraction of the fundamental. (b) Field profiles of an individual channel for the fundamental (upper) and harmonic (lower) guided waves. (c) Dispersion relation for k_z versus k_x for the fundamental. Regions of normal, zero and anomalous diffraction are identified.

in Kerr media [50]. This led to a flurry of activity in photorefractive, liquid crystal and quadratic media [24,51,52]. Here some of the recent progress in quadratic media will be discussed [24,25,53]. All of the work reported to date has been performed in periodically poled PPLN channels arrays, 7 cm long and designed for efficient SHG at 1550 nm.

Discrete quadratic systems consist of parallel, weakly coupled arrays of channel waveguides as shown in Fig. 16(a). The field distributions for the fundamental and harmonic fields for the individual channels are shown in Fig. 16(b). The evanescent tails of the fundamental field overlap the adjacent waveguides which gives rise to weak coupling. On the other hand, the harmonic field is much better confined to the waveguide and there is essentially negligible coupling to the adjacent channels at this frequency. Thus the discrete equations describing the peak channel fields are given by [54]

$$-\mathrm{i}\frac{\mathrm{d}a_n}{\mathrm{d}z} + \beta a_n + C(a_{n+1} + a_{n-1}) + \Gamma a_n^* b_n = 0, \quad -\mathrm{i}\frac{\mathrm{d}b_n}{\mathrm{d}z} + \beta' b_n + \Gamma a_n^2 = 0 \tag{3}$$

Here a_n and b_n are the peak fundamental and harmonic fields in channel n respectively, β and β' are the isolated fundamental and harmonic propagation wave vectors in each channel, C is the inter-channel coupling constant for the fundamental fields and $\Gamma \propto \chi^{(2)}_{\mathrm{eff}}$. Assuming 'plane wave' solutions for the fundamental of the form $\exp[\mathrm{i}\{k_z z + nk_x d\}]$ where k_x is the Block momentum wavevector and $k_x d$ is the relative fundamental phase between adjacent channels, the dispersion relation governing the linear ($\Gamma = 0$) FW propagation in the array is given by $k_z = \beta + 2C\cos(k_x d)$. Fig. 16(c) illustrates this dispersion relation which is periodic in $k_x d$. Since the angle of propagation relative to the z-axis is small, i.e., the inter-channel hopping (discrete diffraction) occurs slowly over a wavelength, the 'discrete' diffraction coefficient by which the fundamental spreads throughout the array is given by $D = \mathrm{d}^2 k_z/\mathrm{d}k_x^2 = -2Cd^2\cos(k_x d)$. As shown in Fig. 16(c), depending on the relative fundamental phase between adjacent channels $k_x d$, the diffraction can be either normal ($D < 0$ for $\pi/2 > |k_x d|$), anomalous ($D > 0$ for $\pi > |k_x d| > \pi/2$) or zero ($D = 0$ for $|k_x d| = \pi/2$). Note that the harmonic is generated separately in each individual channel by the fundamental in that channel.

This diversity in the diffraction phenomenon in such arrays leads to new quadratic solitons that do not exist in continuous media [54,55]. They are found by solving Eqs. (3) including the second order nonlinear coupling between the fundamental and harmonic in each channel. There are two stable solitons, an 'unstaggered' one ($D < 0$) in which all of the channels are excited by fundamental beams in phase, and a 'staggered' discrete soliton ($D > 0$) in which the fundamental phase varies by π from channel to channel. Experimental verification of both is shown in Figs. 17(a) and (b) respectively. The continuous curves are the experimental data where-as the envelope field is described by the discrete points [24]. Note that although the low power diffraction patterns do not necessarily agree with theory, the actual discrete soliton fields agree very well.

A number of new effects have already been observed in such discrete arrays and this is an exciting area for future research [24,25,53,56].

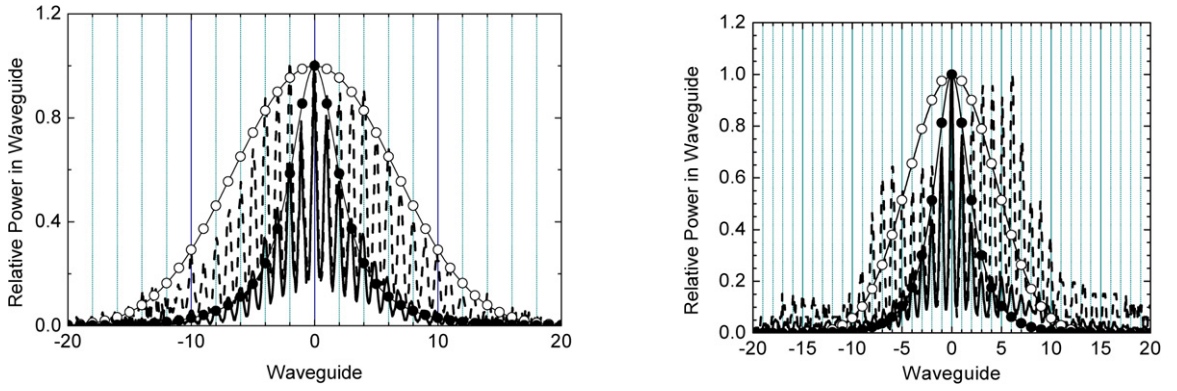

Fig. 17. Excitation of (a) a discrete quadratic unstaggered soliton and (b) a discrete quadratic staggered soliton. Diffracted profiles with open circles calculated and dashed lines measured. Soliton profiles with solid circles calculated and solid line measured.

4. Summary

This review has dealt with a fascinating area of nonlinear interactions via the second order optical nonlinearity $\chi^{(2)}$ involving multiple waves. Under appropriate conditions, solitons are formed, even when only a fundamental beam is injected into a crystal. These quadratic solitons occupy a unique place in soliton science because they consist of two or three different frequency components. This leads to new features such as spatial locking through which all of the components share a common group velocity direction. Furthermore, in contrast to the Kerr 1D case, there are two governing parameters, not just the power but also the linear wavevector mismatch for the components in the soliton structure. These solitons are the eigenmodes of media with second order nonlinearities. As eigenmodes they are very robust and can be excited under input conditions that are far from ideal.

Soliton formation and properties are well-understood in continuous 1D and 2D media. Quadratic solitons in discrete systems represent a new area of research and, although the key experiments may have already been done, solitons involving the interface between a continuous and discrete medium offer an exciting and unexplored area of soliton science. Preliminary results indicate that such solitons can be excited [57].

This review has not included temporal or spatio-temporal solitons. This is currently a very active area being spearheaded by Paolo DiTrapani and colleagues.

Acknowledgements

This research was sponsored by the US National Science Foundation and the Army Office of Research by a MURI.

References

[1] P.A. Franken, A.E. Hill, C.W. Peters, G. Weinreich, Generation of optical harmonics, Phys. Rev. Lett. (1961) 118–120.
[2] N. Bloembergen, Nonlinear Optics, Benjamen, Reading, MA, 1965;
Y.R. Shen, The Principles of Nonlinear Optics, Wiley and Sons, New York, 1984;
F.A. Hopf, G.I. Stegeman, Applied Classical Electrodynamics, vol. 2: Nonlinear Optics, Wiley and Sons, New York, 1986;
R.W. Boyd, Nonlinear Optics, Academic Press, Boston, 1992.
[3] E. Infeld, G. Rowlands, Nonlinear Waves, Solitons and Chaos, Cambridge Univ. Press, Cambridge, 1990;
N.N. Akhmediev, A. Ankiewicz, Solitons, Nonlinear Pulses and Beams, Chapman and Hall, London, 1997.
[4] A. Barthelemy, S. Maneuf, C. Froehly, Propagation soliton et auto-confinement de faisceaux laser par non linearité optique de Kerr, Opt. Comm. 55 (1985) 201–206.
[5] S. Maneuf, F. Reynaud, Quasi-steady state self-trapping of first, second and third order sub-nanosecond soliton beams, Opt. Commun. 66 (1988) 325–329.
[6] J.S. Aitchison, A.M. Weiner, Y. Silberberg, M.K. Oliver, J.L. Jackel, D.E. Leaird, E.M. Vogel, P.W. Smith, Observation of spatial optical solitons in a nonlinear glass waveguide, Opt. Lett. 15 (1990) 471–473.
[7] J.S. Aitchison, K. Al-Hemyari, C.N. Ironside, R.S. Grant, W. Sibbett, Observation of spatial solitons in AlGaAs waveguides, Electron. Lett. 28 (1992) 1879–1880.

[8] P.L. Kelley, Self-focusing of optical beams, Phys. Rev. Lett. 15 (1965) 1005–1008.
[9] J.E. Bjorkholm, A. Ashkin, cw self-focusing and self-trapping of light in sodium vapor, Phys. Rev. Lett. 32 (1974) 129–132.
[10] G. Duree, J.L. Shultz, G. Salamo, M. Segev, A. Yariv, B. Crosignani, P. DiPorto, E. Sharp, R.R. Neurgaonkar, Observation of self-trapping of an optical beam due to the photorefractive effect, Phys. Rev. Lett. 71 (1993) 533–536.
[11] M. Shih, M. Segev, G.C. Valley, G. Salamo, B. Crosignani, P. DiPorto, Observation of two-dimensional steady-state photorefractive screening solitons, Electron. Lett. 31 (1995) 826–827.
[12] M. Peccianti, A. De Rossiu, G. Assanto, A. De Luca, C. Umeton, I.C. Khoo, Electrically assisted self-confinement and waveguiding in planar nematic liquid crystal cells, Appl. Phys. Let. 77 (2000) 7–9.
[13] E.A. Ultanir, G.I. Stegeman, D. Michaelis, F. Lederer, Ch. Lange, Stable dissipative spatial solitons in semiconductor optical amplifiers, Phys. Rev. Lett. 90 (2003) 3903–3906.
[14] Y.N. Karamzin, A.P. Sukhorukov, Nonlinear interaction of diffracted light beams in a medium with quadratic nonlinearity: mutual focusing of beams and limitation on the efficiency of optical frequency convertors, JETP Lett. 20 (1974) 339–342;
Yu.N. Karamzin, A.P. Sukhorukov, Mutual focusing of high-power light beams in media with quadratic nonlinearity, Zh. Eksp. Teor. Phys. 68 (1975) 834–840; Sov. Phys. JETP 41 (1976) 414–420.
[15] L.A. Ostrovskii, Self-action of light in crystals, JETP Lett. 5 (1867) 272–275;
Reviewed in G.I. Stegeman, D.J. Hagan, L. Torner, $\chi^{(2)}$ cascading phenomena and their applications to all-optical signal processing, mode-locking, pulse compression and solitons, J. Opt. Quant. Electron. 28 (1996) 1691–1740.
[16] R. Schiek, Y. Baek, G.I. Stegeman, One-dimensional spatial solitons due to cascaded second-order nonlinearities in planar waveguides, Phys. Rev. E 53 (1996) 1138–1141.
[17] R. Schiek, R. Iwanow, G.I. Stegeman, G. Schreiber, W. Sohler, One-dimensional spatial soliton families in optimally engineered QPM lithium niobate waveguides, Opt. Lett. 29 (2004) 596–598.
[18] W.E. Torruellas, Z. Wang, D.J. Hagan, E.W. VanStryland, G.I. Stegeman, L. Torner, C.R. Menyuk, Observation of two-dimensional spatial solitary waves in a quadratic medium, Phys. Rev. Lett. 74 (1995) 5036–5039.
[19] P. Di Trapani, G. Valiulis, W. Chianglia, A. Adreoni, Two-dimensional spatial solitary waves from traveling wave parametric amplification of the quantum noise, Phys. Rev. Lett. 80 (1998) 265–269.
[20] B. Bourliaguet, V. Couderc, A. Barthelemy, G.W. Ross, P.G.R. Smith, D.C. Hanna, C. De Angelis, Observation of quadratic spatial solitons in periodically poled lithium niobate, Opt. Lett. 24 (1999) 1410–1412.
[21] X. Liu, L.J. Qian, F.W. Wise, Generation of optical spatiotemporal solitons, Phys. Rev. Lett. 82 (1999) 4631–4634.
[22] R. Malendevich, L. Jankovic, S. Polyakov, R. Fuerst, G.I. Stegeman, Ch. Bosshard, P. Gunter, Two-dimensional Type I quadratic spatial solitons in $KNbO_3$ near non-critical phase-matching, Opt. Lett. 27 (2002) 631–633.
[23] H. Kim, L. Jankovic, G.I. Stegeman, S. Carrasco, L. Torner, D. Eger, M. Katz, Quadratic spatial solitons in periodically poled $KTiOPO_4$, Opt. Lett. 28 (2003) 640–642.
[24] R. Iwanow, R. Schiek, G.I. Stegeman, T. Pertsch, F. Lederer, Y. Min, W. Sohler, Observation of discrete quadratic solitons, Phys. Rev. Lett. (2004) 113902.
[25] R. Iwanow, G.I. Stegeman, R. Schiek, T. Pertsch, F. Lederer, Y. Min, W. Sohler, Highly localized discrete quadratic solitons in periodically poled lithium niobate waveguide arrays, Opt. Lett. 30 (2005) 1033–1035.
[26] A.V. Buryak, P. DiTrapani, D. Skryabin, S. Trillo, Optical solitons due to quadratic nonlinearities: from basic physics to futuristic applications, Phys. Rep. 370 (2002) 63–235.
[27] R. Schiek, Y. Baek, G.I. Stegeman, Second harmonic generation and cascading nonlinearity in titanium-indiffused lithium niobate channel waveguides, J. Opt. Soc. Am. B 15 (1998) 2255–2268.
[28] A.V. Buryak, Y.S. Kivshar, Spatial optical solitons governed by quadratic nonlinearity, Opt. Lett. 19 (1994) 1612–1614;
A.V. Buryak, Y.S. Kivshar, Spatial optical solitons governed by quadratic nonlinearity, Opt. Lett. 20 (1995) 1080 (Erratum);
A.V. Buryak, Y.S. Kivshar, Solitons due to second harmonic generation, Phys. Lett. A 197 (1995) 407–412.
[29] C.R. Menyuk, R. Schiek, L. Torner, Solitary waves due to $\chi^{(2)} : \chi^{(2)}$ cascading, J. Opt. Soc. Am. B 11 (1994) 2434–2443.
[30] A.E. Kaplan, Eigenmodes of $\chi^{(2)}$ wave mixings: cross-induced second-order nonlinear refraction, Opt. Lett. 18 (1993) 1223–1225.
[31] G. Assanto, G.I. Stegeman, The simple physics of quadratic spatial solitons, Opt. Express 10 (2002) 388–396.
[32] L. Torner, Stationary solitary waves with second-order nonlinearities, Opt. Commun. 114 (1995) 136–140.
[33] L. Torner, C.R. Menyuk, G.I. Stegeman, Excitation of soliton-like waves with cascaded nonlinearities, Opt. Lett. 19 (1994) 1615–1617;
L. Torner, C.R. Menyuk, G.I. Stegeman, Solitons with second-order nonlinearities, J. Opt. Soc. Am. B 12 (1995) 889–897.
[34] L. Torner, E.M. Wright, Soliton excitation and mutual locking of light beams in bulk quadratic nonlinear crystals, J. Opt. Soc. Am. B 13 (1996) 864–875.
[35] R. Schiek, Y. Baek, G.I. Stegeman, I. Baumann, W. Sohler, One-dimensional quadratic walking solitons, Opt. Lett. 24 (1999) 83–85.
[36] S. Trillo, P. Ferro, Modulational instability in second-harmonic generation, Opt. Lett. 20 (1995) 438–440;
S. Trillo, P. Ferro, Periodical waves, domain walls, and modulational instability in dispersive quadratic nonlinear media, Phys. Rev. E 51 (1995) 4994–4998.
[37] G.I. Stegeman, R. Schiek, H. Fang, R. Malendevich, L. Jankovic, L. Torner, W. Sohler, G. Schreiber, Beam evolution in quadratically nonlinear 1-dimensional media: $LiNbO_3$ slab waveguides, Laser Phys. 13 (2003) 137–147.
[38] H. Fang, R. Malendevich, R. Schiek, G.I. Stegeman, Spatial modulational instability in one-dimensional $LiNbO_3$ slab waveguides, Opt. Lett. 25 (2000) 1786–1788.
[39] A.I. D'yachenko, V.E. Zakharov, A.N. Pushkarev, V.E. Shvets, V.V. Yan'kov, Solitonic turbulence in nonintegrable wave systems, Zh. Eksp. Teor. Fiz. 96 (1989) 2026–2048; Sov. Phys. JETP 69 (1989) 1144–1162.
[40] L. Torner, D. Mihalache, D. Mazilu, E.M. Wright, W.E. Torruellas, G.I. Stegeman, Stationary trapping of light beams in bulk second-order nonlinear media, Opt. Commun. 121 (1995) 149–155.

[41] L. Torner, D. Mazilu, D. Mihalache, Walking solitons in quadratic nonlinear media, Phys. Rev. Lett. 77 (1996) 2455–2458.
[42] S.V. Polyakov, G.I. Stegeman, Existence and properties of quadratic solitons in anisotropic media: variational approach, Phys. Rev. E 66 (2002) 046622.
[43] S. Polyakov, R. Malendevich, L. Jankovic, G.I. Stegeman, Ch. Bosshard, P. Gunter, Effects of anisotropic diffraction on quadratic multi soliton excitation in non-critically phase-matched crystal, Opt. Lett. 27 (2002) 1049–1051.
[44] H. Kim, L. Jankovic, G.I. Stegeman, S. Carrasco, L. Torner, M. Katz, D. Eger, Second harmonic generation, beam dynamics and spatial soliton generation in periodically poled $KTiOPO_4$ (PPKTP), Acta Phys. Polon. 103 (2003) 107–120.
[45] S. Carrasco, S. Polyakov, H. Kim, L. Jankovic, G.I. Stegeman, J.P. Torres, L. Torner, M. Katz, Observation of multiple soliton generation mediated by amplification of asymmetries, Phys. Rev. E 67 (2003), 046616-1.
[46] S. Polyakov, L. Jankovic, H. Kim, G.I. Stegeman, S. Carrasco, L. Torner, M. Katz, Properties of quadratic multi-soliton generation near phase-match in periodically poled potassium titanyl phosphate, Opt. Express 11 (2003) 1328–1337.
[47] L. Jankovic, S. Polyakov, G. Stegeman, S. Carrasco, L. Torner, Ch. Bosshard, P. Gunter, Complex soliton-like pattern generation in Potassium Niobate due to noisy, high intensity, input beams, Opt. Express 11 (2003) 2206–2210.
[48] M. Ohkawa, R.A. Fuerst, G.I. Stegeman, Characteristics of second harmonic generation with quadratic soliton generation versus conventional methods, J. Opt. Soc. Am. B 15 (1998) 2769–2773.
[49] D.N. Christodoulides, F. Lederer, Y. Silberberg, Discretizing light behavior in linear and nonlinear waveguide lattices, Nature 424 (2003) 817–823.
[50] H.S. Eisenberg, Y. Silberberg, R. Morandotti, A.R. Boyd, J.S. Aitchison, Discrete spatial optical solitons in waveguide arrays, Phys. Rev. Lett. 81 (1998) 3383–3386.
[51] J.W. Fleischer, M. Segev, N.K. Efremidis, D.N. Christodoulides, Observation of two-dimensional discrete solitons in optically-induced nonlinear photonic lattices, Nature 422 (2003) 147–151.
[52] A. Fratalocchi, G. Assanto, K.A. Brzdakiewicz, M.A. Karpierz, Discrete propagation and spatial solitons in nematic liquid crystals, Opt. Lett. 29 (2004) 1530–1532.
[53] R. Iwanow, R. Schiek, G.I. Stegeman, T. Pertsch, F. Lederer, Y. Min, W. Sohler, Arrays of weakly coupled, periodically poled lithium niobate waveguide arrays: beam propagation and discrete spatial quadratic solitons, J. Optoelectron. Rev. 13 (2005) 113–121.
[54] T. Peschel, U. Peschel, F. Lederer, Discrete bright solitary waves in quadratically nonlinear media, Phys. Rev. E 57 (1998) 1127–1133.
[55] S. Darmanyan, A. Kobyakov, F. Lederer, Strongly localized modes in discrete systems with quadratic nonlinearity, Phys. Rev. E 57 (1998) 2344–2349;
S. Darmanyan, A. Kamchatnov, F. Lederer, Optical shock waves in media with quadratic nonlinearity, Phys. Rev. E 58 (1998), R4120-3.
[56] R. Iwanow, R. Schiek, G.I. Stegeman, Y. Min, W. Sohler, Discrete modulational instability in periodically poled lithium niobate waveguide arrays, Opt. Express 13 (2005) 7794–7799.
[57] S. Suntsov, K.G. Makris, D.N. Christodoulides, G.I. Stegeman, A. Haché, R. Morandotti, H. Yang, G. Salamo, M. Sorel, Observation of surface discrete solitons, Phys. Rev. Lett. 96 (6) (2006) 063901.